*Revue Paralia, Volume 6 (2013) pp 10.13-10.24*
*Keywords: Wave-current interaction, Reynolds stress, Turbulent viscosity, Code_Saturne*


# A CFD model application to analyze the vertical structure of flow in the wave-current environment

**Maria João TELES [1], Michel BENOIT [2], António A. PIRES-SILVA [1]**

1. Instituto Superior Técnico, ULisboa, Av. Rovisco Pais, 1049-001 Lisbonne, Portugal.
   *mjteles@gmail.com ; aps@civil.ist.utl.pt*
2. Saint-Venant Hydraulics Laboratory, Université Paris-Est (joint research unit between EDF R&D, CETMEF and Ecole des Ponts ParisTech), 6 quai Watier, BP 49, 78401 Chatou Cedex, France.
   *michel.benoit@saint-venant-lab.fr*

**Abstract:**
The nearshore hydrodynamics and coastal circulation result from a variety of phenomena involving complex physical interactions with different scales (large scale circulation currents, tidal effects, waves, wind action, etc.). Among these interactions, we focus on the interaction between waves and currents, especially when the current presents a strong shear over the water depth.
In the present work, the evaluation and analysis of wave-current interactions is made through numerical simulations based on Reynolds Averaged Navier-Stokes (RANS) equations, applied to the modelling of the complete flow motion, namely waves and currents simultaneously (i.e. without decoupling the two phenomena). The advanced CFD solver *Code_Saturne* (ARCHAMBEAU *et al*., 2004) is used for this purpose.
Numerical results are compared with experimental data from UMEYAMA (2005). Four different wave heights and wave periods are tested for each case: (i) waves only, (ii) waves following current and (iii) waves opposing current. A detailed study of the modifications linked to wave-current interactions on vertical profiles of mean horizontal velocities, Reynolds stresses and turbulent viscosities, is presented.

*Received 10 September 2013, accepted 16 October 2013, available online 12 November 2013.*
***Translated version not certified, published under the responsibility of the article authors.***

How to cite the original paper:
TELES M.J., BENOIT M., PIRES-SILVA A.A. (2013). *Application d'un modèle CFD pour analyser la structure verticale de l'écoulement dans un environnement vagues-courant*. Revue Paralia, Vol. 6, pp 10.1–10.12.
DOI:10.5150/revue-paralia.2013.010 (disponible en ligne – http://www.paralia.fr – available online)

## 1. Introduction

The coastal zone has a high degree of complexity due to the wide range of interacting scales, both temporal and spatial, like large scale circulation currents, tidal effects, waves and wind action. The design of coastal protection and harbour sheltering structures, the evaluation of sediment transport and coastal erosion, the assessment of wave power available at a certain spot or the impact of a farm of wave energy converters are examples of possible applications that can benefit from an enhanced knowledge and modelling of these phenomena, and more specifically, of wave-current interaction effects.

The work hereby presented is dedicated to the evaluation and analysis of wave-current interactions at a local scale, by focusing on the vertical profiles of mean horizontal velocity, Reynolds stresses and turbulent viscosity. A numerical model, based on the Reynolds Averaged Navier-Stokes (RANS) equations, is applied to the modelling of the complete flow motion, simultaneously with waves and currents (i.e. without decoupling the two phenomena).

The numerical results were compared with laboratory data obtained by UMEYAMA (2005). Vertical profiles of mean horizontal velocities and Reynolds stresses were obtained for four different test conditions: current only, waves only, waves following current and waves opposing current.

The organization of this paper is as follows: after the introductory section, the experimental data used are described in section 2; section 3 presents the numerical model and its settings; section 4 discusses the results and the findings of the work; conclusions are summarized in section 5.

## 2. Experimental data

UMEYAMA (2005) performed a series of experiments in a 25 m long channel, 0.7 m wide and with a water depth of 0.2 m. Regular waves were generated with a piston type wave maker. Four wave heights and wave periods were tested (labelled T1 to T4) with waves only, waves following currents and waves opposing currents. The mean current velocity in the channel was about 12 cm/s, both in the direction of the waves and in the opposite direction. The forced wave parameters are listed in Table 1 for each test case. The vertical profiles of mean velocity and Reynolds stresses were measured by a laser Doppler anemometer at a distance of 10.5 m from the wave generator.

*Table 1. Wave height and wave period for the four test cases*

| ***Tests*** | ***T1*** | ***T2*** | ***T3*** | ***T4*** |
|---|---|---|---|---|
| ***Wave height (m)*** | *0.0202* | *0.0251* | *0.0267* | *0.0280* |
| ***Wave period (s)*** | *0.9* | *1.0* | *1.2* | *1.4* |

In view of the range of wave heights and water depths set in UMEYAMA (2005)'s experiments, an approximate value of $H/h \approx 0.1$ was found, which qualifies them as intermediate non linear waves. With dimensionless depth $kh \approx 0.1$, these experiments are typically characterized as intermediate water depths.

## 3. *Code_Saturne* model

In the numerical simulations, the RANS CFD solver *Code_Saturne*, developed at Electricité de France (EDF) (ARCHAMBEAU *et al*., 2004) was used. The RANS equations are written in a conservative form and then integrated over the control volumes of each cell of the three-dimensional (3D) mesh.

$$\frac{\partial \rho}{\partial t} + div(\rho u) = 0 \tag{1}$$

$$\rho \frac{\partial u}{\partial t} + div\left(\rho u \otimes u\right) = div(\sigma) + S_u \tag{2}$$

$\rho$ is the fluid density, $u$ the fluid velocity vector, $\sigma$ the viscous stress tensor and $S_u$ an additional momentum source term to be defined by the user. For a turbulent flow, the stress tensor $\sigma$ includes the effect of pressure, viscous stress $\tau$, and the turbulent Reynolds stress tensor $R_{ij}$.

In order to close the system of equations (1) and (2), the turbulent Reynolds stress tensor $R_{ij}$ has to be modelled and somehow related to mean flow. *Code_Saturne* has implemented a number of turbulence closure models. In this study, a Reynolds Stress Model (RSM) was chosen, namely the $R_{ij}$-$\varepsilon$ SSG model (SPEZIALE et al., 1991). In Reynolds Stress Models (RSM) a Reynolds stress transport equation (3) accounts for the directional effects of the Reynolds stress fields and, therefore, dispenses with the eddy viscosity hypothesis. There are also six transport equations for the six independent components of the Reynolds stress tensor and one equation for the dissipation rate $\varepsilon$.

$$\rho \frac{\partial R_{ij}}{\partial t} + \nabla.\left(\rho u R_{ij} - \mu grad R_{ij}\right) = P_{ij} + G_{ij} + \Phi_{ij} + d_{ij} - \rho \varepsilon_{ij} \tag{3}$$

$$\rho \frac{\partial \varepsilon}{\partial t} + \nabla.\left(\rho u \varepsilon - \mu grad\, \varepsilon\right) = d_{\varepsilon} + C_{\varepsilon 1} \frac{\varepsilon}{k}\left[P + G_{\varepsilon}\right] - \rho C_{\varepsilon 2} \frac{\varepsilon^2}{k} \tag{4}$$

$R_{ij}$ represents the Reynolds stress tensor, $P_{ij}$ and $G_{ij}$ are the turbulence production tensors related to mean shear stresses and gravity effects respectively, $\Phi_{ij}$ is the pressure strain term, $d_{ij}$ and $d_{\varepsilon}$ the turbulent diffusion terms and $\varepsilon_{ij}$ the dissipation term (considered isotropic) (ARCHAMBEAU et al., 2004).

*Code_Saturne* is able to model free surface flows by using the Arbitrary Lagrangian Eulerian (ALE) method (ARCHAMBEAU et al., 1999), which ensures an accurate representation of the free surface variations. The RANS equations then gain a new term, which is the vertical velocity of the mesh. At each time step the mesh is updated accordingly.

About 20 cells per wavelength had to be guaranteed for mesh generation to get a good representation of the wave propagation. On the other hand, the mesh resolution cannot be too fine next to the moving wall to avoid mesh crossover and divergence of the simulation. A structured and hexahedral mesh was created with a constant resolution in the $x$ direction of 120 cells over a length of 30 m ($\Delta x \approx 0.25$m), one single cell in the $y$ (transversal) direction and a variable number in the vertical direction $z$. In the latter, a geometric progression of the vertical mesh size $\Delta z$ ranging from 0.002 m (near the bottom) to 0.005 m (near the free surface), (cf. figure 1) was adopted.

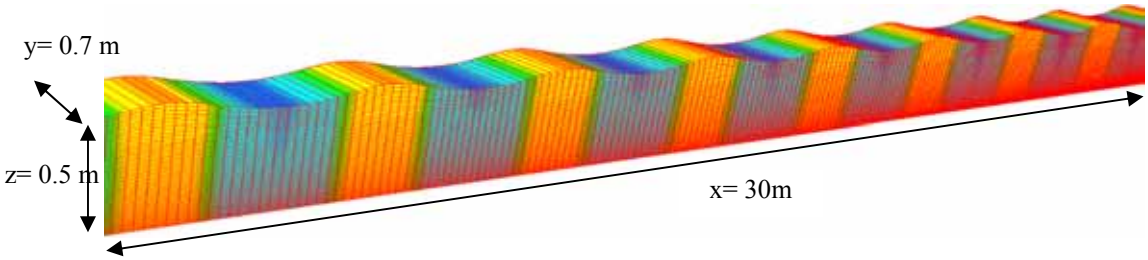


*Figure 1. Computational domain representative of experiments from UMEYAMA (2005).*

To minimize undesirable super and sub-harmonic free waves, a second order displacement of a piston type wave board (DEAN & DALRYMPLE, 1991) was applied on the channel at the left lateral boundary (figure 1). *Code_Saturne* was forced simulating a horizontal movement of the mesh on the upwave wall. The signal had to be progressively imposed at this boundary to avoid a sudden horizontal movement of the mesh and thus, mesh crossover. The wave reflections at the right end of the channel were dealt with by an artificial beach based on a viscous damping term that increased linearly from the bottom to the free surface.

The numerical solution is strongly dependent on the correct imposition of the boundary conditions. An additional condition (5) proposed by CELIK & RODI (1984), relative to the turbulence closure scheme, had to be imposed on the free surface.

$$\varepsilon = \frac{k_w^{3/2}}{\alpha h} \tag{5}$$

$\varepsilon$ is the turbulent dissipation, $k_w$ the turbulent kinetic energy at the water surface, $\alpha = 0.18$ an empirical constant and $h$ the water depth. In the case of the RSM model, $k$ is computed as half the trace of the Reynolds stress tensor: $k = ½(R_{xx} + R_{yy} + R_{zz})$.

With this condition, the turbulent dissipation increases and the eddy viscosity decreases towards the free surface. This behaviour was observed in the experiments made by NEZU & RODI (1986).

## 4. Results and discussions

As specified in Section 2, the experiments from UMEYAMA (2005) were made with different wave heights and periods. It should be noted that these experiments do not include a blocking situation of the waves by the current.

The conditions of Table 1 for the four cases were tested in *Code_Saturne*. In the following, for current only case, comparisons between numerical results and data are shown for the vertical profiles of the mean horizontal velocity, the Reynolds stress $R_{xz}$ (figure 2), the dimensionless turbulent kinetic energy and the dimensionless dissipation rate (figure 3). The same comparisons were made for tests T1 and T4, for waves only (figure 4), waves following current (figure 5) and waves opposing current (figure 6).

It was first considered to be the current only test case. It can be seen on figure 2 that both the vertical profiles of their mean horizontal velocity and Reynolds stress are well reproduced by *Code_Saturne*.

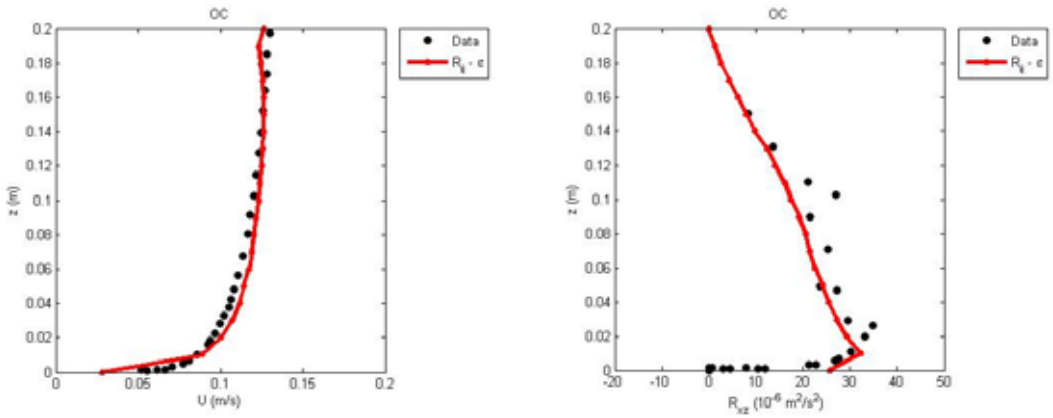


*Figure 2. Vertical profiles of mean horizontal velocity (on the left) and Reynolds stress $R_{xz}$ (on the right) for current only.*

The dimensionless turbulent kinetic energy and the dimensionless dissipation rate are shown below with for the "current only" case (figure 3). Semi-empirical formulas (NEZU & NAKAGAWA, 1993) were also included for the "current only" case and used to estimate the dimensionless turbulent kinetic energy (6) and dissipation rate (7).

$$\frac{k}{u_*^2} = 4.78e^{(-2z/h)} \tag{6}$$

$$\frac{\varepsilon h}{u_*^3} = 9.8\left(\frac{z}{h}\right)^{-1/2} e^{(-3z/h)} \tag{7}$$

We can observe that the comparison of the numerical simulations with the semi-empirical curves shows, in general, the same order of magnitude throughout the water depth.

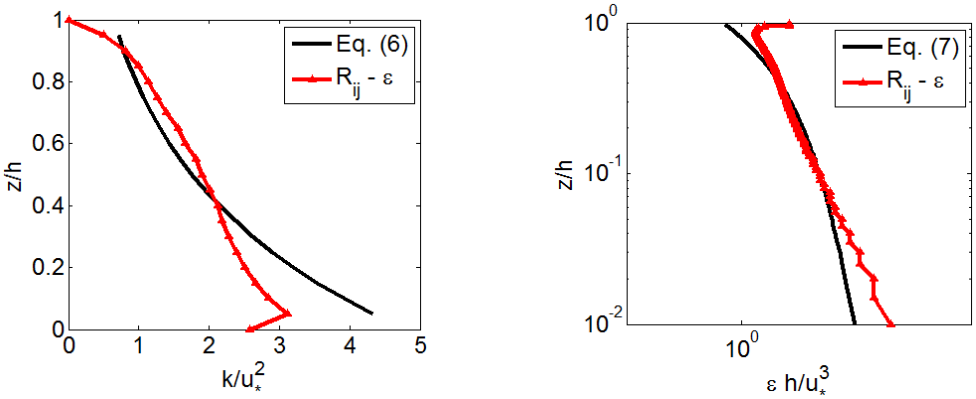


*Figure 3. Vertical profiles of the dimensionless kinetic turbulent energy and turbulent dissipation for "current only" (i.e. no waves).*

Figure 4 shows the vertical profile of the mean horizontal velocity for two different wave heights and periods, and without any current. The numerical model predicts reasonably well the magnitude of the mean horizontal velocity, although differences are observed on the shape of the vertical distribution. To compensate the mass flux induced by wave propagation in the region between the wave trough and wave crest, a negative current, opposed to wave propagation, appears.

The following set of two figures (figures 5 and 6) represent the vertical profile of mean horizontal velocities for waves superimposed in a turbulent current. For waves co-following a current (figure 5), and comparing with the current only profile (from figures 5 to 9: OC=current only, which corresponds to the tests with current only, without waves), an increase of the velocity near the bed followed by its reduction near the free surface is observed in the measurements. Both these effects are well reproduced by the model. The other wave heights and periods tested (not shown) exhibit a similar behaviour (TELES *et al*, 2013).

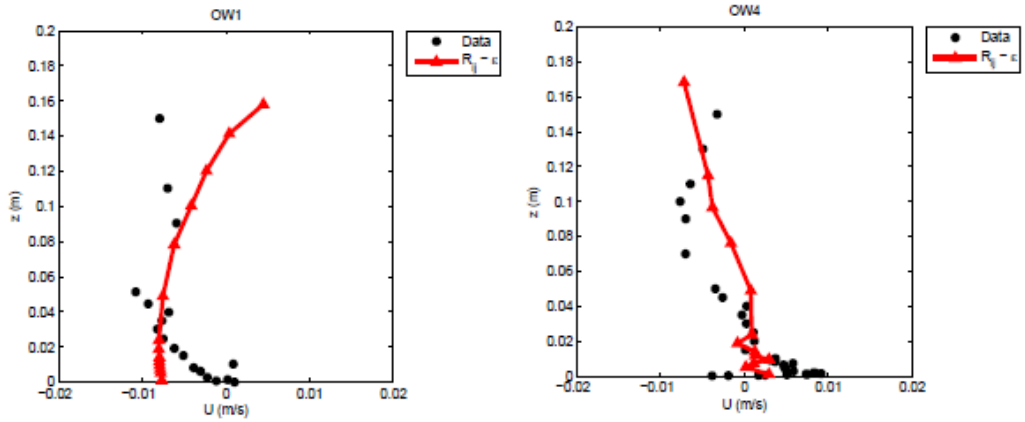


*Figure 4. Vertical profile of mean horizontal velocity for waves only: OW1 (H=0.0202 m; T=0.9 s) and OW4 (H=0.0280 m; T=1.4 s).*

The phase averaged Reynolds stresses induced by the waves represent a phase averaged correlation between the horizontal and vertical velocities. As pointed out by OLABARRIETA *et al.* (2010), in intermediate water depths, like in these experiments, as the wave height increases, so does this correlation, and a greater reduction of the mean horizontal velocity should be noticed. However, as the wave period increases, the vertical component of the particle motion decreases, causing a reduction of Reynolds stresses. The effects of the wave height and wave period act in opposing directions and could explain why the reduction near the surface for waves following the current does not change much across the experiments.

For waves opposing currents (figure 6), the main observed feature is the increase of the velocity shear near the free surface. Again, the numerical simulations follow closely the experimental data.

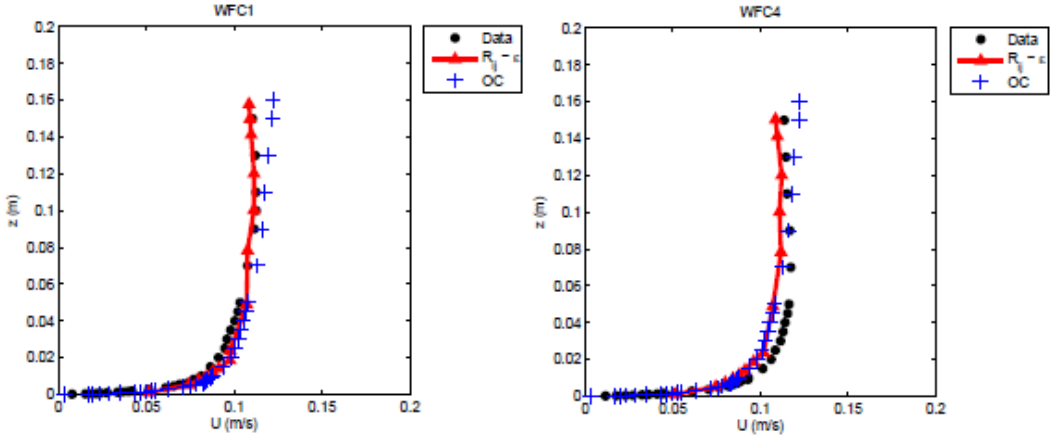


*Figure 5. Vertical profile of mean horizontal velocity for waves following current: WFC1 (H=0.0202 m; T=0.9 s) and WFC4 (H=0.0280 m; T=1.4 s).*

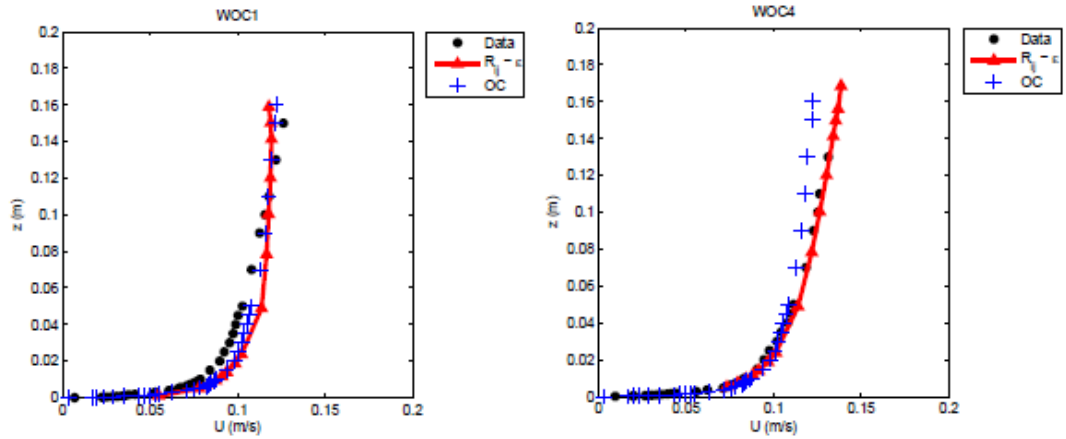


*Figure 6. Vertical profile of mean horizontal velocity for waves opposing current: WOC1 (H=0.0202 m; T=0.9 s) and WOC4 (H=0.0280 m; T=1.4 s).*

Figures 7 and 8 present the vertical profile of the Reynolds stress $R_{xz}$. The maximum value of this Reynolds stress decreases when compared with the current only case, independently of the direction between the waves and the current. The superimposition of waves causes a reduction of Reynolds stresses, not only near the bottom, but also throughout the water depth. This general trend is also observed in the model results. In the WFC4 case, a discrepancy in the simulated Reynolds stresses near the surface in comparison to the experimental measurements can be seen. In particular, the reverse in sign of the measurements close to $z = 0.06$ m does not show up in the model simulations. The observed differences could be a consequence of not considering a non-zero shear stress at the free surface due to the interface between air and water (DORE, 1978).

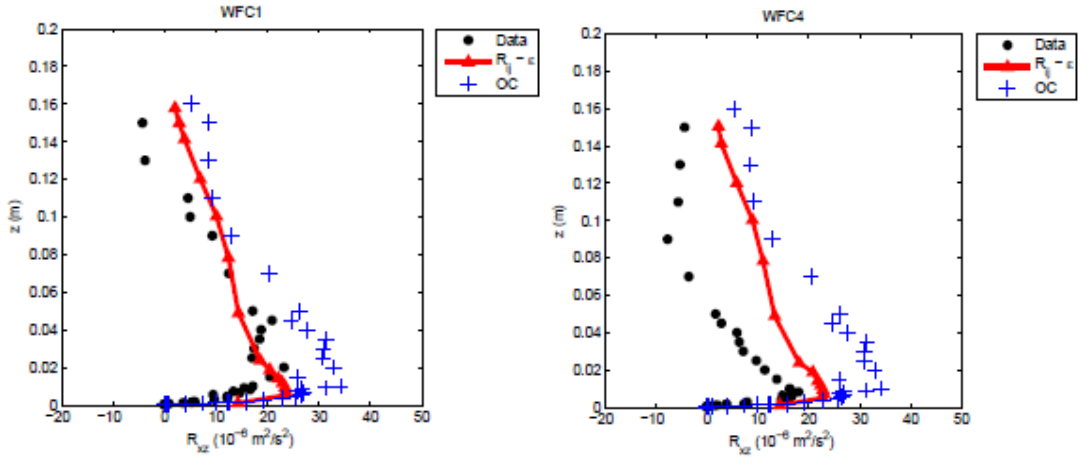


*Figure 7. Vertical profile of Reynolds stress $R_{xz}$ for waves following current: WFC1 (H=0.0202 m; T=0.9 s) and WFC4 (H=0.0280 m; T=1.4 s).*

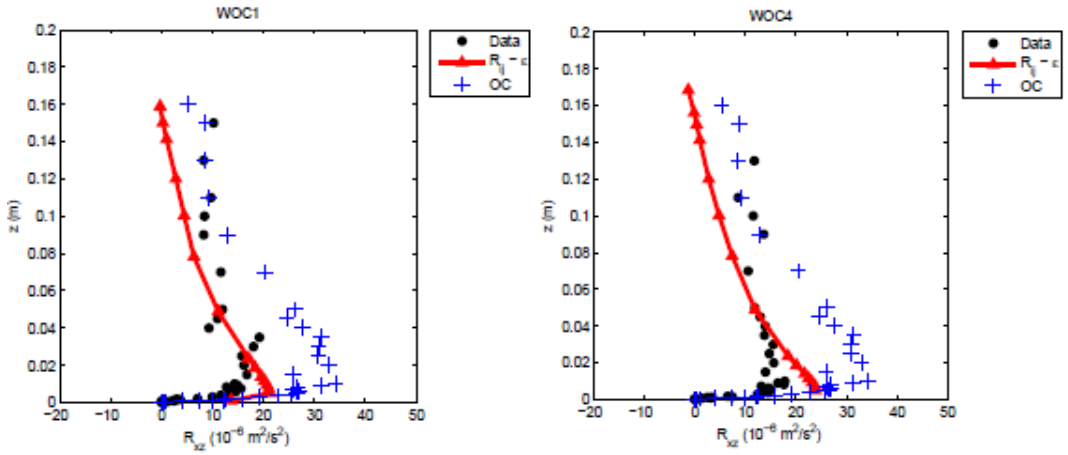


*Figure 8. Vertical profile of Reynolds stress $R_{xz}$ for waves opposing current: WOC1 (H=0.0202 m; T=0.9 s) and WOC4 (H=0.0280 m; T=1.4 s).*

Overall, the comparisons between *Code_Saturne* simulations and the data of UMEYAMA (2005) showed a good agreement and the specifics of the wave-current interactions at this local scale can be accounted for.

The experiments of NEZU & RODI (1986) allowed to estimate the vertical profile of the turbulent viscosity in the current only case. Comparing with *Code_Saturne* results, the same order of values was obtained for the dimensionless viscosities (figure 9). The turbulent viscosity is zero, both at the bottom and on the moving free surface. To achieve this kind of behaviour at the free surface, the boundary condition for the turbulent dissipation, expressed by (5), was essential.

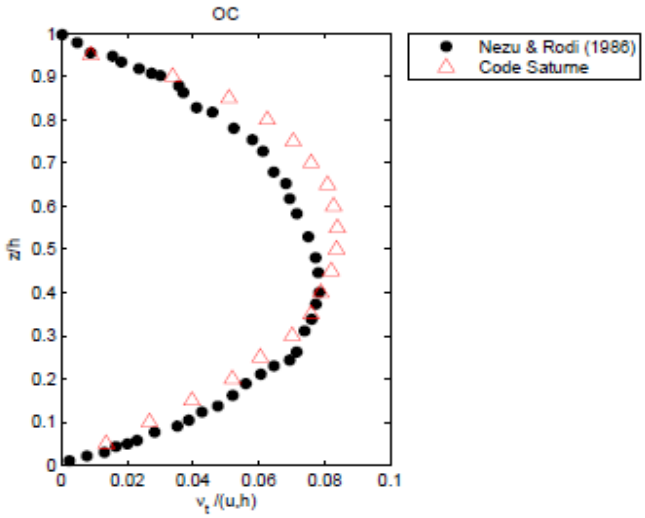


*Figure 9. Comparison between measured and calculated eddy viscosity profile for an open channel flow with current only.*

This analysis of the turbulent viscosity profile was repeated with the waves superimposed on the current for the different values of the wave height and period, as in UMEYAMA (2005), and the calculations are shown in figure 10. The general shape of the turbulent viscosity profile does not change much when compared with the "current only" profile. Note that HUANG & MEI (2003) have also considered a parabolic and continuous profile when dealing with smooth bottoms.

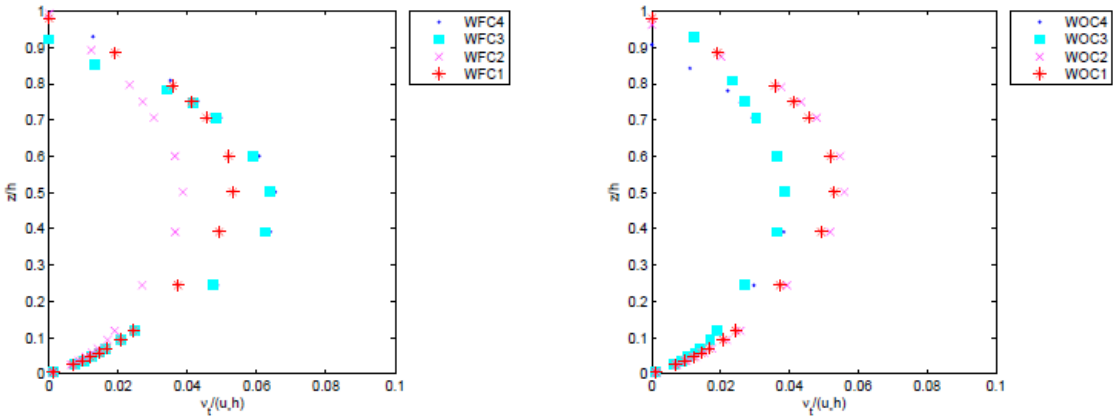


*Figure 10. Vertical profiles of non-dimensional turbulent viscosity obtained by Code_Saturne by using the $R_{ij}$–ε SSG turbulence closure model for tests with different wave heights and wave periods for "waves following current" cases (WFC, left panel) and "waves opposing current" cases (WOC, right panel).*

The similarity of the vertical profile of the non-dimensional turbulent viscosity observed in this set of experiments can be used to devise a simple parameterisation of the turbulent viscosity in such wave-current combined flows that could then be used as input in more simplified numerical models. To obtain this parameterisation of the turbulent viscosity development over the water column, with waves and current, a dimensionless relation between the turbulent viscosity ($\nu_t$), gravity ($g$), mean velocity ($U$), water depth ($h$), wave period ($T$), wave length ($L$) and wave height ($H$) has been tested. After considering several possible dependences, it was found that the non-dimensional turbulent viscosity $\nu_t/(gUT^2)$ at each relative distance from the bottom ($z/h$) seemed to decrease approximately linearly with the Ursell number ($HL^2/h^3$), as illustrated in figure 11, where the various variables depicted corresponded to the simulations made with *Code_Saturne*. It should be stressed that this tentative parameterization of the turbulent viscosity needs to be validated against a more extensive set of data.

The relations obtained and represented in figure 11 (equation 8) can be used to deduce a relationship between the non-dimensional turbulent viscosity versus relative distance from the bottom.

$$\frac{\nu_t}{gUT^2}\left(z/h\right)=\left[1\times10^{-5}Ur-2\times10^{-4}\right]\left(\frac{z}{h}\right)^2+\left[-1\times10^{-5}Ur+2\times10^{-4}\right]\left(\frac{z}{h}\right)+\left[1\times10^{-7}Ur+2\times10^{-6}\right] \quad (8)$$

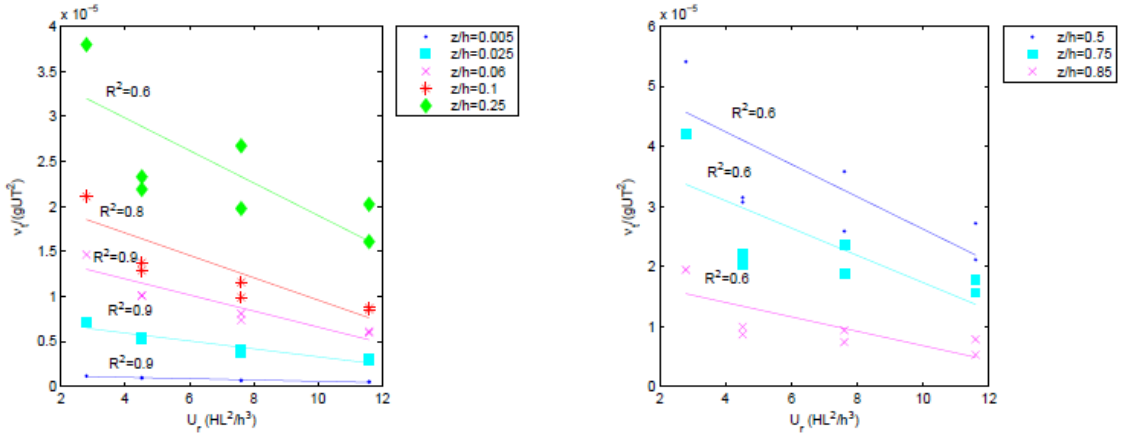


*Figure 11. Variation of the non-dimensional turbulent viscosity $\nu_t/(gUT^2)$ for each z/h level as a function of the Ursell number $Ur = HL^2/h^3$.*

## 5. Conclusions

The modelling capabilities of the *Code_Saturne* model were verified for free surface flows in a combined wave-current environment. Data from UMEYAMA (2005) experiments were used to evaluate performance of the model. Different test cases were available: currents only, waves only, waves following currents and waves opposing currents. The change of the vertical profile of the mean horizontal velocity caused by the presence of following or opposing waves on the mean flow was well reproduced. When waves are superimposed in the same direction as the current there is a significant reduction of the mean velocities near the free surface, while when waves have opposite direction to the current, the shear of the velocity profile increases.

The Reynolds stress profile changes were also checked for the combined wave and current environment. It can be concluded, that regardless of the direction of the waves (following or opposing the current), a change of the bed shear stress shows up. The superimposition of waves causes a reduction of turbulence stresses, not only near the bottom, but also throughout the water column.

Finally, the expression for the turbulent dissipation at the free surface, proposed by CELIK & RODI (1984), imposed at the free surface, has shown to be essential to reproduce correctly the vertical profiles of the Reynolds turbulent stresses and the turbulent viscosity.

As the $R_{ij}$–ε turbulence closure model offers the great advantage of solving both the turbulent dissipation and Reynolds stresses, it was also attempted to propose a parameterization of the profile over the water depth of the turbulent viscosity as a function of the Ursell number.

## 6. References

ARCHAMBEAU F., GUIMET V., BASTIN G. (1999), *Application du prototype de module ALE du Solveur Commun à des cas de surface libre,* Technical report EDF HE-41/99/054/A, EDF Research and Development, Chatou, France.

ARCHAMBEAU F., MECHITOUA N., SAKIZ M. (2004). *Code_Saturne: a finite volume code for the computation of turbulent incompressible flows - Industrial applications*. International Journal on Finite Volumes, Vol. 1(1), pp 1-62.

CELIK I., RODI W. (1984). *Simulation of free surface effects in turbulent channel flows*. Physicochemical Hydrodynamics, Vol. 5, pp 217-227.

DEAN R.G., DALRYMPLE R.A. (1991). *Water wave mechanics for engineers and scientists*. Singapore, World Scientific Press. doi:10.1142/9789812385512

DORE B.D. (1978). *Some effects of the air-water interface on gravity waves.* Geophysics Astrophysics Fluid Dynamics, Vol. 10, pp 215-230.

NEZU I., RODI W. (1986). *Open channel flow measurements with a laser Doppler anemometer*. Journal of Hydraulic Engineering, Vol. 112 (5), pp 335-355. doi:10.1061/(ASCE)0733-9429(1986)112:5(335)

NEZU I., NAKAGAWA H. (1993). *Turbulence in open-channel flows,* A.A. Balkema, Rotterdam. CRC Press.

OLABARRIETA M., MEDINA R., CASTANEDO S. (2010). *Effects of wave-current interaction on the current profile.* Coastal Engineering, Vol. 57 (7), pp 643-655. doi:10.1016/j.coastaleng.2010.02.003

SPEZIALE C.G., SARKAR S, GATSKI T.B. (1991). *Modeling the pressure-strain correlation of turbulence: an invariant dynamical systems approach*. Journal of Fluid Mechanics, Vol. 227, pp 245-272. doi:10.1017/S0022112091000101

TELES M.J., PIRES-SILVA A.A., BENOIT M. (2013). *Numerical modelling of waves and current interactions at a local scale,* Ocean Modelling, Vol. 68, pp 72-87. doi:10.1016/j.ocemod.2013.04.006

UMEYAMA M. (2005). *Reynolds stresses and velocity distributions in a wave–current coexisting environment*. Journal of Waterway, Port, Coastal and Ocean Engineering, Vol. 131 (5), pp 203–212. doi:10.1061/(ASCE)0733-950X(2005)131:5(203)